ChemComm

Cite this: *Chem. Commun.*, 2011, **47**, 9732–9734

www.rsc.org/chemcomm

COMMUNICATION

Stable aluminium fluoride chelates with triazacyclononane derivatives proved by X-ray crystallography and ^{18}F-labeling study†

Dinesh Shetty,[ab] Soo Young Choi,[c] Jae Min Jeong,*[ab] Ji Youn Lee,[ab] Lathika Hoigebazar,[ab] Yun-Sang Lee,[ab] Dong Soo Lee,[a] June-Key Chung,[ab] Myung Chul Lee[a] and Young Keun Chung[c]

Received 28th May 2011, Accepted 11th July 2011
DOI: 10.1039/c1cc13151f

A single crystal structure of an aluminium-fluoride complex of a model compound (NODA-benzyl) was studied to understand the co-ordination chemistry. Series of ligands with an extra carboxylic acid linker for biomolecule conjugation were studied for improved ^{18}F-labeling applications.

Positron emission tomography (PET) is an important imaging modality for assessing neurologic, oncologic and cardiologic abnormalities.[1–3] ^{18}F is the most widely used PET radioisotope because of excellent imaging properties, and thus, the development of ^{18}F-labeled bioactive molecules has become an important area.[4–7]

Most established ^{18}F-labeling procedures start with the trapping of the [^{18}F]fluoride ion on an anion-exchange resin and subsequent elution with an organic/aqueous solution containing base that can act as a phase-transfer catalyst.[8] The eluate is then dried to activate the [^{18}F]fluoride. ^{18}F-labeling is performed using a nucleophilic substitution reaction in organic solvent with heating in the presence of a base catalyst. Finally, the organic solvent is removed for clinical application. However, this general procedure has inherent problems in the labeling of biomolecules, because radiolabeling in organic solvent at high temperature detrimentally affects biomolecules such as peptides, proteins, and nucleic acids. Furthermore, the drying steps required are time consuming and make automation of the procedure difficult. Thus, the developments of new methods without drying steps are actively being pursued.[9–11]

A novel method for the one step ^{18}F-labeling of peptides using $(Al–^{18}F)^{+2}$ complex formation with 1,4,7-triazacyclononane-1,4,7-triacetic acid (NOTA) derivatives has been reported, which did not need a drying step neither before nor after the labeling.[12–14] It was an important progress in ^{18}F-labeling chemistry, but structural studies on complexes of aluminium fluoride and NOTA derivatives were not conducted to determine how the chelating agent structures are related to labeling efficiency.

It has been reported that Al^{3+} binds with F^- more strongly than sixty other metal ions tested,[15] and forms a much stronger complex with F^- than with any other halide.[16] Generally, most halides form more stable complexes with Fe^{3+} than with Al^{3+}, but F^- binds to Al^{3+} 10 times more strongly than to Fe^{3+}.[17]

In the present study, we determined the chemical structure of an Al–^{19}F-1,4,7-triazacyclononane-1,4-diiacetic acid (NODA)-benzyl complex (**6**) using X-ray crystallography, and synthesized various NODA derivatives containing different linkers suitable for subsequent conjugation to biomolecules (Fig. 1, Scheme S1, ESI†).‡ *In vitro* and *in vivo* stabilities and biodistribution studies were performed on the labeled complexes using mice.

The common building block compound **1** was synthesized from 1,4,7-triazacyclononane by reacting with *tert*-butyl-bromoacetate. Purification of reaction products by column chromatography gave a mixture of mono-, di-, and tri-substituted products. This mixture was purified using a pH controlled workup method. NODA was obtained by acid

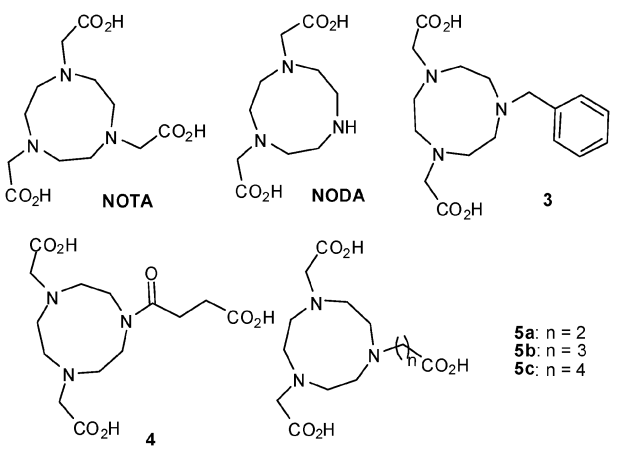

Fig. 1 Chemical structures of NOTA, NODA and derivatives.

[a] *Department of Nuclear Medicine, Department of Radiation Applied Life Science and Institute of Radiation Medicine, Seoul National University College of Medicine, Seoul, Korea. E-mail: jmjng@snu.ac.kr*
[b] *Clinical Research Institute and Cancer Research Institute, Seoul National University Hospital, Seoul, Korea*
[c] *Intelligent Textile System Research Center and Department of Chemistry, Seoul National University, Seoul, Korea*

† Electronic supplementary information (ESI) available: Experimental methods, spectroscopic data and detailed crystallographic data. CCDC 813724. For ESI and crystallographic data in CIF or other electronic format see DOI: 10.1039/c1cc13151f

hydrolysis of **1**. Nucleophilic substitution of **1** with benzyl bromide and succinic anhydride followed by acid hydrolysis gave **3** and **4** as hydrochloride salts, respectively. Furthermore, a series of derivatives containing various acid linkers (**5a–c**), which could be used for conjugation to biomolecules *via* active ester formation, were synthesized to determine relations with labeling yields. Compound **5a** was prepared by reacting **1** with 3-bromopropionic acid and subsequent acid hydrolysis, whereas **5b** and **5c** were synthesized by reacting **1** with protected 4-bromobutyric acid or 5-bromovaleric acid and subsequent hydrolysis using lithium hydroxide, respectively.

We examined the solid state structure of complex **6** by single crystal X-ray analysis. The model complex **6** was obtained by reacting **3** with $AlCl_3$ in sodium acetate buffer (pH 3.5), followed by addition of NaF under heating (Fig. S1, ESI†). Complex formation was confirmed by a molecular ion peak by mass/ion spray positive ionization (MS/ESI^+) analysis and the complex was purified by reverse phase high performance liquid chromatography (RP-HPLC). Single crystals were obtained by evaporating a solution of pure **6** from a water:EtOH mixture (1 : 9, v/v) at 4 °C. X-Ray crystallography data are summarized in Table S1 (ESI†).

The $(Al–F)^{2+}$ ion fits well inside the nitrogen/oxygen coordination cavity of **3**. The results obtained confirmed that five 5-membered rings are composed around the coordinated central aluminium atom on which a fluorine atom is bonded covalently (Fig. 2). The complex forms a discrete monomer and was found to have a distorted geometry due to the restricted fixation of the chelating ligands. The nitrogen atom attached to the benzyl group was also found to participate in the chelation. The coordination includes three nitrogen atoms occupying one face and two oxygen atoms of carboxylate occupying the opposite face. Distortion of the coordination from the regular octahedral shape was evidenced by the compression of N–Al(1)–N angles (83.30°) and the expansions of O(1)–Al(1)–O(3) (96.94(7)°), F(1)–Al(1)–O(3) (98.56(7)°) and F(1)–Al(1)–O(1) (93.69(7)°) angles from the expected 90°. As a result, the *trans* angles of N(1)–Al(1)–O(3), N(2)–Al(1)–F(1) and N(3)–Al(1)–O(1) were 165.61(8)°, 174.28(7)° and 165.71(7)°, respectively. The average Al–N bond length was 2.083 Å, which is slightly longer than that in the Al–NOTA complex (average Al–N = 2.06 Å),[18] possibly due to bonding between the aluminium and the fluorine atom. The average Al–O bond length was 1.86 Å, which is comparable to that of Al–NOTA complex (average Al–O distance = 1.84 Å). The Al(1)–F(1) bond length was 1.709(14) Å, which is similar to the calculated bond length for the ground state of diatomic Al–F.[19] This value indicates the strong coordination bond formation between the aluminium and fluoride. Three intra- and inter-molecular hydrogen bonds were observed (Fig. S3, ESI†) between O(1) and O(11) (2.8718(31) Å), O(2) and O(12) (2.8653(38) Å), and O(11) and neighboring O(12_1) (2.8114(38) Å).

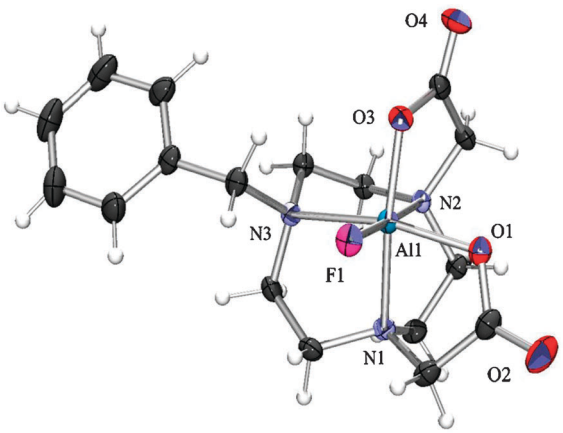

Fig. 2 Crystal structure of complex **6**. Selected bond lengths [Å] and angles [°]: Al(1)–N(1) 2.0497(18), Al(1)–N(2) 2.0863(19), Al(1)–N(3) 2.1125(18), Al(1)–O(1) 1.8856(16), Al(1)–O(3) 1.8446(16), Al(1)–F(1) 1.7090(14), N(1)–Al(1)–N(2) 82.89(7), N(1)–Al(1)–N(3) 83.66(7), N(2)–Al(1)–N(3) 83.34(7), O(3)–Al(1)–O(1) 96.94(7), F(1)–Al(1)–O(1) 93.69(7), F(1)–Al(1)–O(3) 98.56(7).

To study ^{18}F labeling, we first compared NOTA and NODA at different concentrations and pH. $^{18}F^-$ was prepared as previously described,[10] and $(^{18}F–Al)^{2+}$ was prepared by mixing Al^{3+} (11 to 180 nmol) with $^{18}F^-$ in 1.0 mL of sodium acetate buffer (0.1 M, pH 4) at room temperature for 10 min. Each ligand (12.5 to 200 nmol) was mixed with the $(^{18}F–Al)^{2+}$ solution and reactions were monitored at room temperature and 110 °C after 10 min. Labeling efficiencies were determined using Instant Thin Layer Chromatography-Silica Gel (ITLC-SG) and labeled products were purified using an Alumina-N cartridge (Fig. 3a). Purities were also checked by autoradiography (Fig. S2, ESI†). The labeling efficiencies of NOTA and NODA at room temperature were only 0 and 1.28%, respectively,

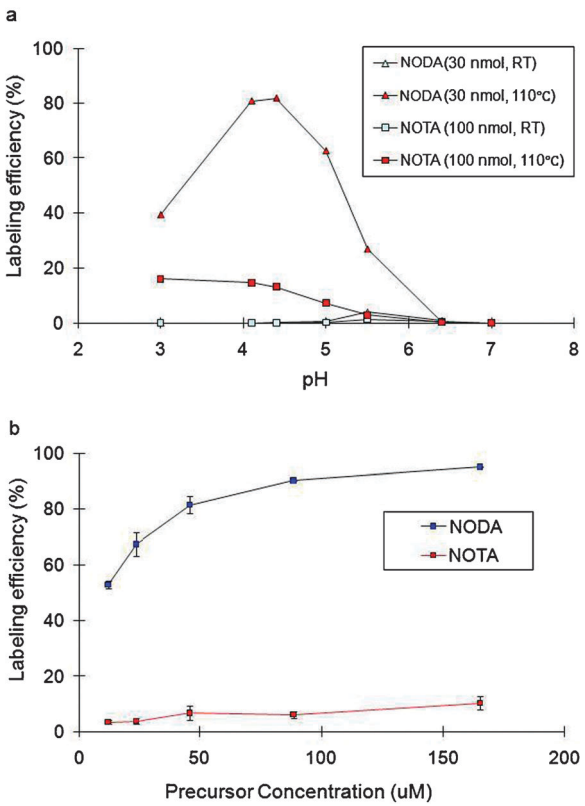

Fig. 3 Comparative labeling efficiencies under different reaction conditions. (a) At different pH values and reaction temperatures. (b) At different chelator concentrations.

Table 1 Al–^{18}F labeling of various ligands[a]

Labeled compound	R group	Labeling efficiency[b] (%)
NODA	–H	89.3 ± 2.3
3	$-CH_2Ph$	83.0 ± 7.7
4	$-CO(CH_2)_2CO_2H$	32.9 ± 6.1
5a	$-(CH_2)_2CO_2H$	23.6 ± 7.7
5b	$-(CH_2)_3CO_2H$	86.1 ± 2.1
5c	$-(CH_2)_4CO_2H$	77.8 ± 3.4
NOTA	$-CH_2CO_2H$	10.9 ± 0.4

[a] NODA derivatives were labeled with $(Al–^{18}F)^{2+}$ at a concentration of 50 nM in sodium acetate buffer (pH 4) at 110 °C for 10 min. [b] Determined by ITLC: expressed as radioactivity percentage of the product areas *versus* total areas.

but these increased up to 16% and 89% at 110 °C, respectively. The optimal pH range for labeling was between 4.1 and 4.4 (Fig. 3a). Ligand concentration also was an important factor for labeling efficiency (Fig. 3b). High concentrations of **2** and NOTA (165 μM) gave maximum labeling yields (95% and 10%, respectively), and these decreased to 52% and 3%, respectively, when their concentrations were reduced to 11 μM. NODA consistently showed higher labeling efficiency than NOTA demonstrating that the presence of the third carboxylic group in NOTA compared to NODA interferes the binding of fluoride to aluminium.

Five more NODA derivatives were synthesized to identify ligands that improve labeling yield (Scheme S1, ESI† and Table 1). Using the procedure described above, these ligands (50 nM) were labeled with ^{18}F at pH 4. Compound **5a**, which has an ethyl spacer between the backbone ring and the carboxylic acid group showed lower labeling efficiency (23.6%) than **5b** having a propyl (86.1%) or **5c** having a butyl (77.8%) spacer. The low yield of **5a** is probably due to interference of the propionic carboxylic acid during complex formation. Thus, Al^{3+} can form stable complex **5a**, which hinders the coordination bonding between $^{18}F^-$ and chelated Al. A similar phenomenon is observed for NOTA. This observation suggests that butyric or valeric acid substitutes would give high labeling efficiencies.

In the present study, it was found that if the substituent at the 2° amine of NODA can form a 5- or 6-membered ring with Al^{3+}, then fluoride binding yield to Al^{3+} decreased. However, if it cannot form a ring or can form greater than a 6-membered ring, fluoride binding was not seriously affected. This is also supported by the fact that the labeling efficiencies of **2** (no substituent) and **3** (benzyl substituent) are high because their substituents cannot form rings with aluminium (Table 1).

However, compound **4** showed a low labeling efficiency, despite the fact that it cannot form a 6-membered ring. We believe that this is due to the presence of a carbonyl group adjacent to a substituted nitrogen atom, which could give a negative effect for the formation of a stable complex due to the electron-withdrawing effect.

Both ^{18}F–Al–NODA and ^{18}F–Al–**3** were found to be stable in human serum at 37 °C and in sodium acetate buffer (pH 4) at room temperature for at least 2 h (Fig. S4, ESI†). Protein binding studies were performed after incubating the labeled compounds with human serum at 37 °C. All the compounds studied showed very low protein binding at 60 min (0.23 ± 0.06% for ^{18}F–Al–NODA, 0.06 ± 0.01% for ^{18}F–Al–**3**, and 0.79 ± 0.12% for ^{18}F–Al–**5b**). This result suggests the possibility of using these compounds for *in vivo* studies.

Biodistribution studies on ^{18}F–Al–**3** and ^{18}F–Al–**5b** in balb/c mice showed low bone uptakes, which confirmed stabilities *in vivo* (Fig. S5 and S6, ESI†). ^{18}F–Al–**3** and ^{18}F–Al–**5b** were rapidly cleared from blood (~9% at 60 min) and showed low residual activities in tissues. The high uptake and low retention in kidneys indicated excretion *via* the renal route. However, ^{18}F–Al–**3** showed high uptakes in the liver and kidneys, indicating excretion *via* both the renal and hepatobiliary routes. It is clear that the negative charge of ^{18}F–Al–**5b** and the lipophilic benzyl group of ^{18}F–Al–**3** make these differences in biodistribution.

In summary, this study shows how fluoride is bound to aluminium in F–Al–NODA using X-ray crystallography, and describes the results of ^{18}F-labeling studies using newly synthesized ligands. It demonstrates that the existence of a competing intra-molecular ligand which can form a 5- or 6-membered ring is an important factor for binding fluoride to aluminium.

We acknowledge support from Converging Research Center Program (2009-0082087) and NRL grant (R0A-2008-000-20116-0) from MEST.

Notes and references

‡ Crystal data for $C_{17}H_{23}Al_1F_1N_3O_4{\cdot}2H_2O$ (293 K): M = 415.40, monoclinic, space group $P2_1/a$, a = 13.9007(6) Å, b = 7.1927(5) Å, c = 19.9931(12) Å, β = 106.473(3)°, V = 1916.93(19) Å^3, Z = 4, $\rho_{calc.}$ = 1.439 g cm^{-3}, absorption coefficient = 0.156 mm^{-1}, total reflections collected 7515, unique 4371 (R_{int} = 0.0471), GOF = 1.008, R_1 = 0.0499, R_w = 0.1051 ($I > 2\sigma(I)$).

1 R. Cohen, *Mol. Imaging Biol.*, 2007, **9**, 204–216.
2 N. Oriuchi, T. Higuchi, T. Ishikita, M. Miyakubo, H. Hanaoka, Y. Iida and K. Endo, *Cancer Sci.*, 2006, **97**, 1291–1297.
3 A. Zhu and H. Shim, *Eur. J. Nucl. Med. Mol. Imaging*, 2011, **45**, 1–14.
4 J. McAfee and R. Neumann, *Nucl. Med. Biol.*, 1996, **23**, 673–676.
5 H. Wester, K. Hamacher and G. Stöcklin, *Nucl. Med. Biol.*, 1996, **23**, 365–372.
6 Y. S. Chang, J. M. Jeong, Y. S. Lee, H. W. Kim, G. B. Rai, S. J. Lee, D. S. Lee, J. K. Chung and M. C. Lee, *Bioconjugate Chem.*, 2005, **16**, 1329–1333.
7 G. E. Smith, H. L. Sladen, S. C. G. Biagini and P. J. Blower, *Dalton Trans.*, 2011, **40**, 6196–6205.
8 K. Hamacher, H. Coenen and G. Stocklin, *J. Nucl. Med.*, 1986, **27**, 235.
9 J. Aerts, S. Voccia, C. Lemaire, F. Giacomelli, D. Goblet, D. Thonon, A. Plenevaux, G. Warnock and A. Luxen, *Tetrahedron Lett.*, 2010, **51**, 64–66.
10 H. W. Kim, J. M. Jeong, Y. S. Lee, D. Y. Chi, K. H. Chung, D. S. Lee, J. K. Chung and M. C. Lee, *Appl. Radiat. Isot.*, 2004, **61**, 1241–1246.
11 B. Y. Yang, J. M. Jeong, Y. S. Lee, D. S. Lee, J. K. Chung and M. C. Lee, *Tetrahedron*, 2011, **67**, 2427–2433.
12 P. Laverman, W. McBride, R. Sharkey, A. Eek, L. Joosten, W. Oyen, D. Goldenberg and O. Boerman, *J. Nucl. Med.*, 2010, **51**, 454.
13 W. McBride, C. D'Souza, R. Sharkey, H. Karacay, E. Rossi, C. Chang and D. Goldenberg, *Bioconjugate Chem.*, 2010, **21**, 1331.
14 W. McBride, R. Sharkey, H. Karacay, C. D'Souza, E. Rossi, P. Laverman, C. Chang, O. Boerman and D. Goldenberg, *J. Nucl. Med.*, 2009, **50**, 991.
15 A. Bond, G. Hefter, I. U. o. Pure and A. C. C. o. E. Data, *Critical survey of stability constants and related thermodynamic data of fluoride complexes in aqueous solution*, Pergamon Press, 1980.
16 B. Martin, *Coord. Chem. Rev.*, 1996, **149**, 23–32.
17 R. Martin, *J. Inorg. Biochem.*, 1991, **44**, 141–147.
18 A. Jyo, T. Kohno, Y. Terazono and S. Kawano, *Anal. Sci.*, 1990, **6**, 629–630.
19 E. Muniz and F. Jorge, *Int. J. Quantum Chem.*, 2006, **106**, 943–951.

